energies

MDPI

Article

Evaluation and Analysis of Selective Deployment of Power Optimizers for Residential PV Systems

Kostas Sinapis [1,2,*], Konstantinos Tsatsakis [1,2], Maarten Dörenkämper [1] and Wilfried G. J. H. M. van Sark [2]

[1] Netherlands Organization for Scientific Research (TNO), 5656 AE Eindhoven, The Netherlands; kostas_ts@hotmail.com (K.T.); maarten.dorenkamper@tno.nl (M.D.)
[2] Copernicus Institute of Sustainable Development, Utrecht University, 3564 CB Utrecht, The Netherlands; w.g.j.h.m.vansark@uu.nl
* Correspondence: kostas.sin@hotmail.com

Abstract: Partial shading is widely considered to be a limiting factor in the performance of photovoltaic (PV) systems applied in urban environments. Modern system architectures, combined with per module deployment of power electronics, have been used to improve performance, especially at heterogeneous irradiance conditions, but they come with a high investment cost. In this paper, another approach is used to evaluate the selective deployment of power optimizers (SDPO), which can operate with a variety of string inverters and can be retrofitted in PV systems suffering from high shading losses. A combination of modelling and outdoor field testing showed the benefits and drawbacks of SDPOs in a variety of shading scenarios. Results suggest that there is an energy yield increase of 1–2% on an annual basis compared to that of a reference system. The exact level of increase depends on the shading patterns and combination scenarios used in this paper.

Keywords: BIPV; power optimizers; SDPO; partial shading

Citation: Sinapis, K.; Tsatsakis, K.; Dörenkämper, M.; van Sark, W.G.J.H.M. Evaluation and Analysis of Selective Deployment of Power Optimizers for Residential PV Systems. *Energies* **2021**, *14*, 811. https://doi.org/10.3390/en14040811

Academic Editor: Andrii Chub
Received: 5 January 2021
Accepted: 1 February 2021
Published: 4 February 2021

1. Introduction

Penetration of solar photovoltaic (PV) systems worldwide is forecasted to increase in the next years [1]. More specifically, the implementation of building applied (BAPV) and building integrated (BIPV) systems is expected to have a pivotal role in the energy transition efforts of governments worldwide, especially in countries where land is expensive or is used for agricultural purposes. The technical potential of PV systems installed on existing and suitable roofs has been extensively researched by several authors, with promising results [2–4]. In the US, building roofs can host a total of 1118 GW of PV capacity, resulting in a potential generation of 1432 TWh annually. The latter represents approximately 39% of total electricity sector sales. In The Netherlands, which is a densely populated country, the roof potential reaches 892 km^2 of suitable PV roofs and thus can cover 98% of total Dutch household electricity demands. It seems obvious that in order to achieve such an imperative task, the losses of PV systems have to be kept to a minimum. In an urban environment, roofs and terraces are often affected by shade due to the close proximity of buildings, poles, antennas, and dormers, which introduce electrical and thermal mismatches.

Cells in PV modules are connected in series and, therefore, partially shaded cells can be forced to support current levels exceeding their characteristic short-circuit current. As a result, they become reverse biased and act as an external load, consuming the power produced by other solar cells. Consequently, the output power of the module is decreased and, when modules are connected in a series configuration (which is typical in residential and commercial applications), the power losses are exaggerated and non-linear. The most heavily shaded cells limit the current and power that can be extracted from the system at the maximum power point (MPP) operating voltage. Moreover, the large power dissipation in the shaded cells results in local overheating (resulting in a "hot spot") [5] and can have permanent destructive effects on the PV module.

Nowadays, most PV modules are equipped with bypass diodes to prevent power consumption from shaded cells and to prevent hot spots. By utilizing bypass diodes, the higher currents of the unshaded cell strings can flow around the shaded cell string and, hence, the panel can continue to supply power at a reduced voltage rather than provide no power at all. Although it would be ideal to have one diode integrated for each cell [6], at present this solution is not economically feasible. Typically, in a module with 60 mono- or multi-crystalline silicon cells, three bypass diodes are used, one for each 20 cell-substrings. Therefore, the use of bypass diodes comes at the expense of losing the output of the unshaded cells that are skipped over.

Module level power electronics (MLPE) are devices that are attached to individual modules in order to increase performance under shaded conditions by performing maximum power point tracking (MPPT) at the module level. Generally, these products fall into the categories of power optimizers (PO), AC micro-inverters, or the relatively new concept of hybrid devices that combine the key advantages of power optimizers and micro-inverters [7].

Power optimizer and micro-inverter systems have been proven to mitigate partial shading losses [8] when compared to a single string inverter system, but both solutions come with an extra cost for the whole system. Finding a way to mitigate mismatch and partial shading losses at a low cost has attracted the interest of several researchers, e.g., [9,10]. In the above context, installing power optimizers at panels that experience the most shading in a system (selective deployment) is a relatively new solution that has been proposed. In Figure 1, the approach of selective deployment of PO (SDPO) can be compared with other approaches.

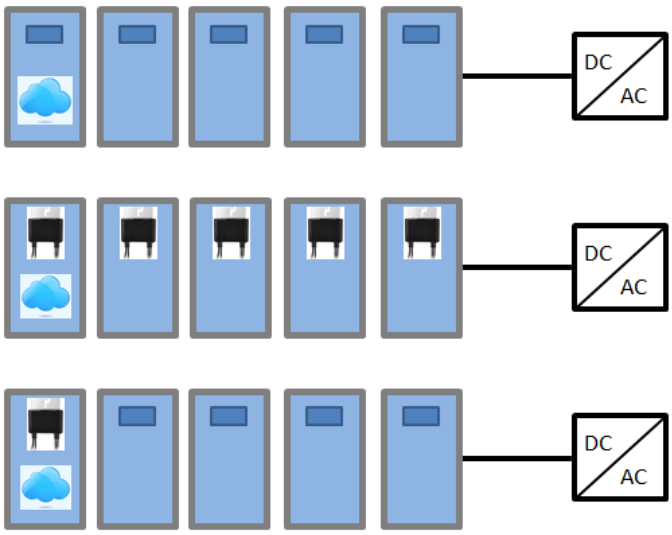

Figure 1. The top displays a string inverter system without any module level power electronics (MLPE), the middle displays a typical power optimizer (PO) system, with optimizers deployed behind each individual solar panel, and the bottom displays selective deployment of a PO in the partially shaded panel only.

Power optimizer manufacturers claim that significant gains can be achieved by selective deployment of PO (SDPO) in residential PV applications that experience losses due to partial shading while keeping investment costs down compared to micro-inverters or the full application of power optimizers. This is of paramount importance in order to maximize energy gain for a considerable lower cost. In this paper, modeling and experimental analysis are conducted to present the potential benefits of selective deployment of power optimizers.

2. Methodology

2.1. Field Testing of SDPO in Realistic Conditions

On the roof of the "Vertigo" building of the Technical University Eindhoven, two identical PV systems with 35° inclination and 180° azimuth (south orientation) have been installed. Each system consists of six Yingli Panda 265 Wp [11] panels connected in series to a Sunny Boy 1.5 kW string inverter [12]. The panels are composed of 60 series connected mono-crystalline n-type silicon solar cells. Every sub-string of 20 cells is assigned to one bypass diode connected anti-parallel across the cells. The field test setup can be seen in Figure 2. In one of the PV systems, buck-type power optimizers were installed in two consecutive panels (panel 1 and panel 2). The panels' numbering was set from right to left for all systems. The system located at the right in the front is a conventional string inverter system and was used as a reference system during the field test. The global horizontal and the in-plane irradiance at the field-test site were measured with two ISO standard pyranometers, while module and ambient temperature were measured with T-type thermocouples. The DC and AC electrical parameters of each PV system were monitored through a WT1800 high performance power analyzer from Yokogawa Japan with ±0.1% basic power accuracy [13]. The irradiance, the temperature, and the electrical parameters were synchronized and stored with a MW100 data acquisition system from Yokogawa Japan at one-minute resolution.

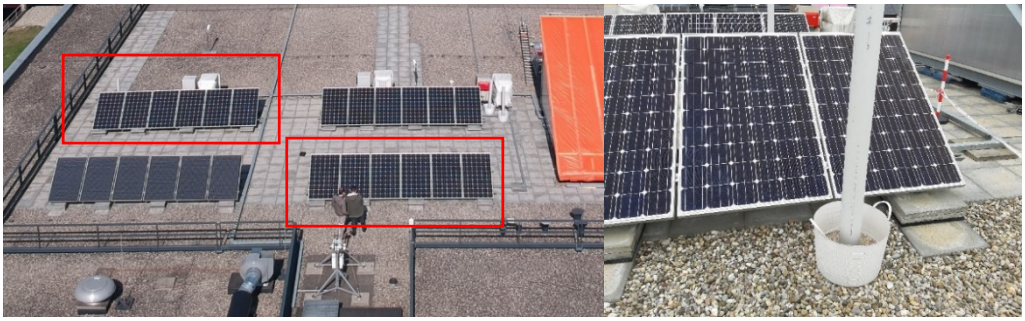

Figure 2. Drone picture of the two PV systems used for field testing (**left side**) and a shading element between two panels (**right side**).

To evaluate the selective deployment of power optimizers, the performance of the two different systems was compared under the same shading conditions. Two identical poles with 146 cm height and 12.3 cm diameter were used as a shading object during the field test. The poles were placed at the exact same position between panel 1 and panel 2 (Figure 2) for all four systems to provide equal shading among the different setups.

2.2. Yield Simulation Model

A yield simulation model, which was developed in previous work [14], has been adapted to accommodate the selective deployment of power optimizers. The complete PV performance (python-based) model for this research is comprised of six different models integrated into one: A 3D SketchUp model, a shading model, an effective irradiance model, a temperature model, a current and voltage (I-V) model, and a system loss model. A flowchart of the complete modelling procedure for the yield simulations can be seen in Figure 3. The evaluation of the selective deployment of POs is based on the simulation results for a set of different shading scenarios during a typical meteorological year (TMY) in Eindhoven, The Netherlands. A field test of a reference and SDPO system was utilized to fine tune the simulation model.

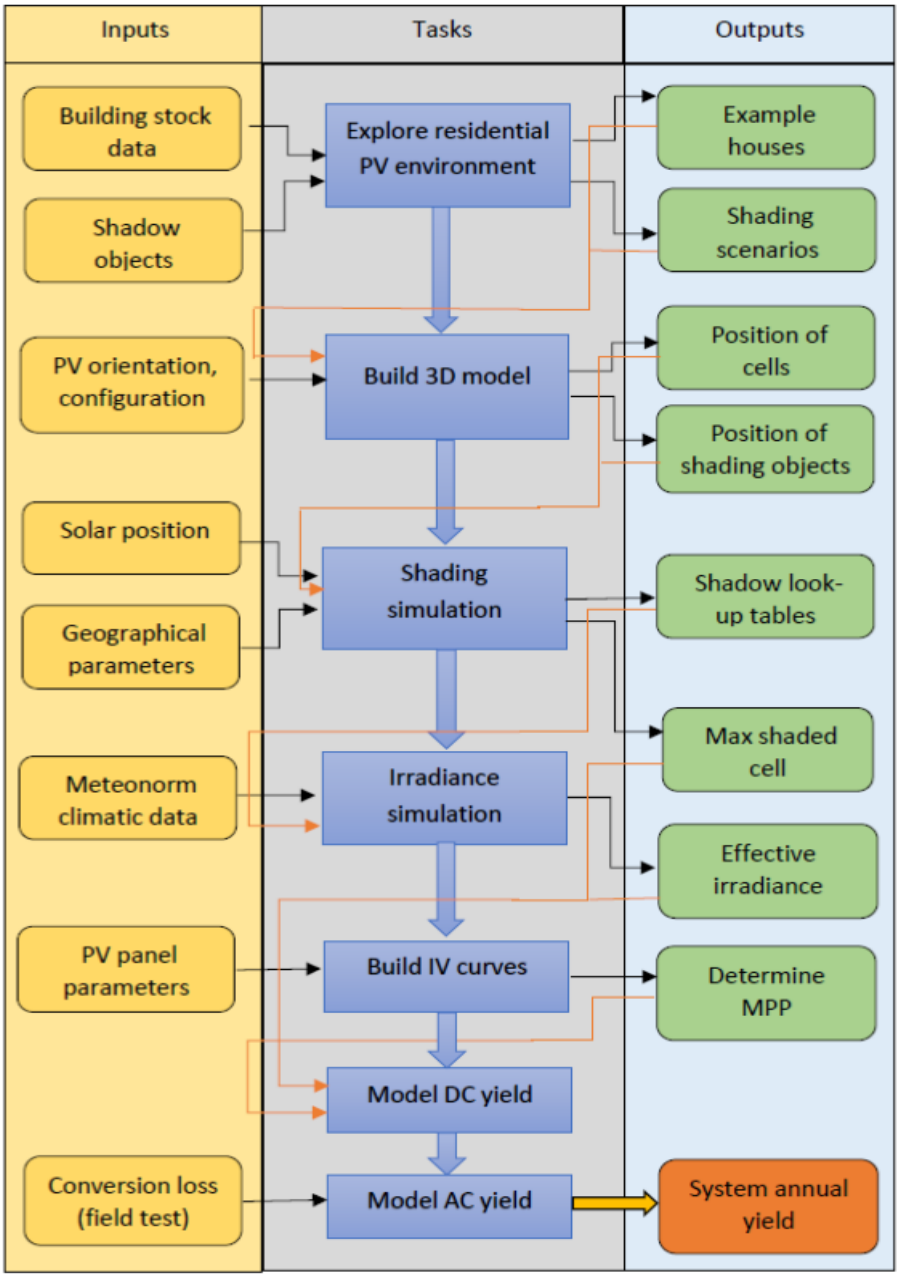

Figure 3. Flowchart of the simulation model.

2.3. Shading Scenarios

The most recent results from a housing research study (which is conducted every three years by the Dutch government) show that row (terraced) and detached houses are the dominant types of housing in the residential building stock [15], comprising more that 65% of the total stock (42.4% and 23% respectively). Therefore, in this research, these two types were selected in order to build representative models for the residential PV systems in The Netherlands.

SketchUp representations of the two systems have been constructed and can be seen in Figure 4, Aside from providing the opportunity to determine the location of the edge points of all objects of interest in 3D space, this software can produce very accurate designs, reinforcing the quality of the shading analysis.

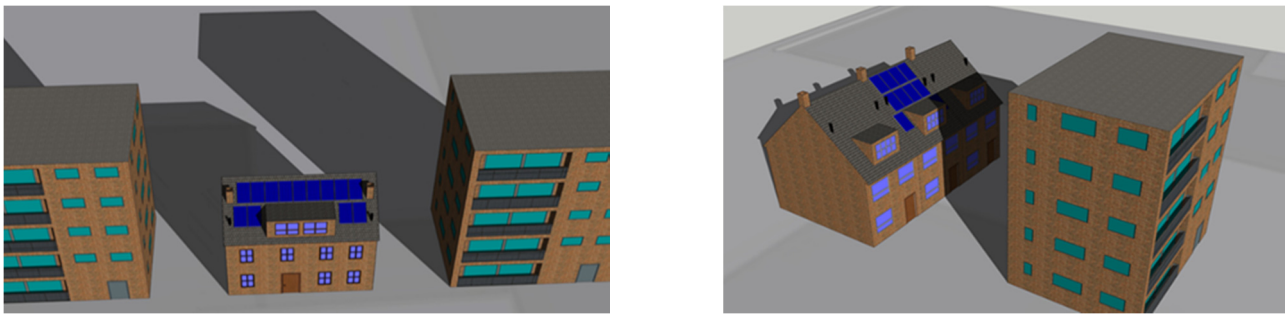

Figure 4. Representation of the two house scenarios in SketchUp, detached house on the (**left side**) and row house on the (**right side**).

Partial shading conditions on roof mounted PV system can be caused by several different objects and conditions, such as chimneys, exhaust pipes (poles), trees, nearby buildings, bird droppings, soiling, etc. For this research, four types of shading objects were selected for the modeling process: chimneys, exhaust pipes, dormers and the shading caused by a nearby building. These are the most common types met in the Dutch residential environment. Moreover, only the shadows from opaque objects were considered for this study. To evaluate the performance of the power optimizers under aggressive shading scenarios, the dimensions for the different shading objects were selected to be above the average of the typical constructions that are met in the Dutch-built environment.

For the scope of the research, seven different shading scenarios were simulated for each system:

- Reference scenario: No shading objects present. This scenario was built due to the need for control comparisons.
- Exhaust pipes (or pole) scenario: Only exhaust pipes were present for the roof of each system (two for the detached case, six for the row house case).
- Chimneys scenario: Only chimneys were present as shading objects (two for the detached case, one for the row house case).
- Dormer scenario: The shading effect of the dormer was examined (one for the detached case, three for the row house case).
- Nearby buildings (or building) scenario: Shading was caused only by the apartment blocks present in each system (two for the detached case, one for the row house case).
- Heavy (or all) shading scenario: The effect of all the different types of shading objects at the same time for each case was explored.
- Medium shading scenario: Selected shading objects were present on each system. For the detached house case, one building, one dormer, one pipe, and one chimney were used, while for the terraced house case, one dormer, three pipes, and one chimney were used.

3. Results

3.1. SDPO Operation

SDPOs are usually DC–DC buck converters. The principle of operation is to reduce the voltage of the panel and "match" the module output current with the string current. In this way, the total string current is not affected by modules operated under partially shaded conditions. The SDPO can operate with a variety of inverters and is not bonded with specific inverter technologies and brands. This makes the use of SDPO perfectly suited for the retrofit market. Each SDPO has its own maximum power point tracker (MPPT), which does not interfere with the MPPT of the string inverter. When no partial shading or other mismatch is present, the SDPO simply conducts and, hence, avoids high efficiency losses due to conversion. In this way, the overall efficiency of the SDPO is kept at very high levels. Another point of attention is the fact that manufacturers of SDPO suggest that

the shade optimization function of various inverter brands (Optitrac, Shadow mode, etc.) should be deactivated in case their inverter is combined with SDPOs.

Figure 5 shows the operation of a SDPO in real time in comparison to a string inverter system, which is not optimized. The yellow dotted line denotes the input voltage (actual V_{MPP} of the panel as detected by the SDPO), the red line denotes the output voltage, and the black line denotes the voltage on the same panel (under the same pole shading) at the reference system. The shade from the pole is at panel 2 early in the morning and moves gradually to panel 1 at around noon. When the panel is not shaded, no conversion occurs at the DC–DC converter and a conduction state is achieved. While without shade the voltage of the reference and optimized module are very similar, when partial shading occurs, the string inverter of the reference system is able to bypass groups of solar cells, thus limiting the voltage output. The input voltage of the SDPO due to partial shading is very high, indicating operation on a local maximum power point. In the output, a large voltage reduction can be seen, which is comparable with the reference module's voltage.

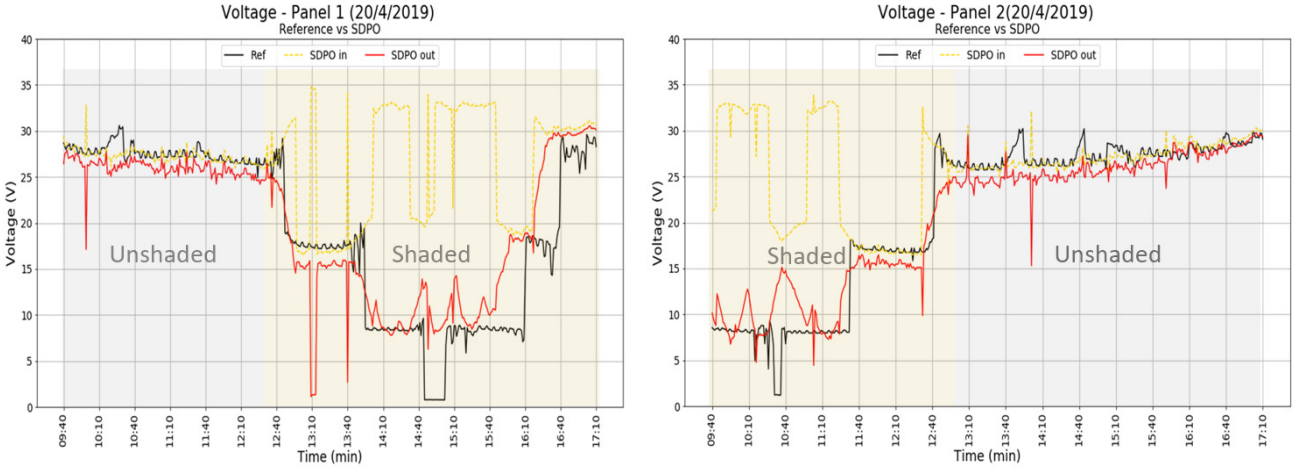

Figure 5. Voltage input and output of the optimized module versus the reference module, which is connected in a string of six modules.

In Figure 6, the current of the SDPO and the reference system can be seen. The output current for the two systems is almost identical, while a delay in detecting the MPP for the reference system can be seen (sharp dips in the left hand plot). Significant DC yield gains (+4.2%) are observed for the system with POs when the shade from the pole falls on the panels with SDPOs installed.

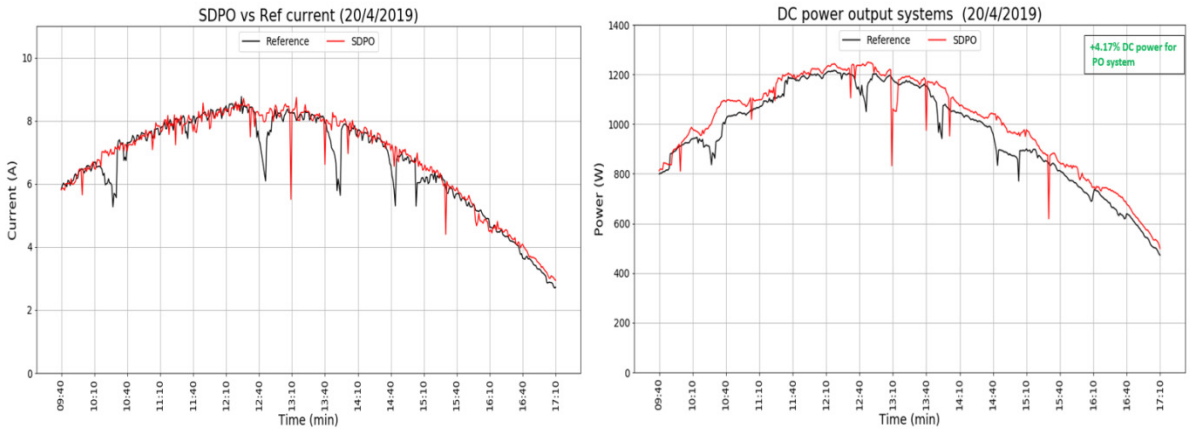

Figure 6. Current and DC power curves of optimized and non-optimized modules during a sunny day under partial shading from a pole.

While there is a small improvement in terms of power throughout the day for the optimized panels, the opposite is true when partial shading is present on panels for which the power is not optimized by SDPOs. Therefore, it is critical at the design phase of the PV system to identify the potentially shaded panels beforehand and optimize accordingly. In Figure 7, the output of the reference and SDPO optimized system can be seen. As long as the un-optimized panel 3 is partially shaded, the output power of the reference system is higher than that of the SDPO system.

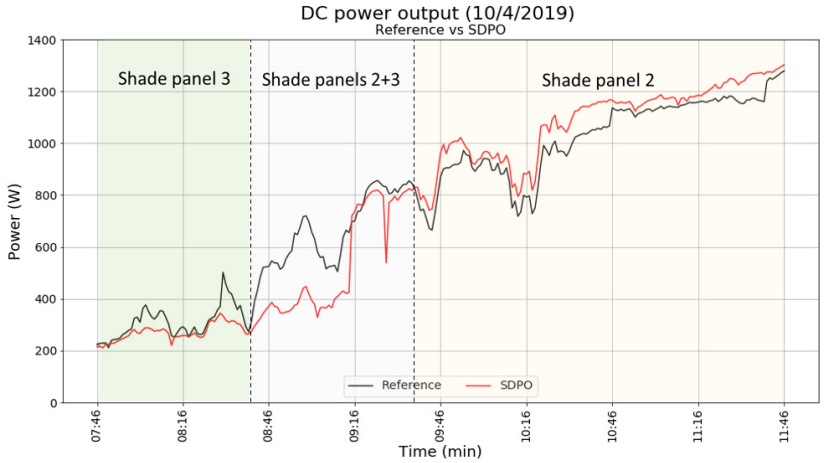

Figure 7. Comparison of the output of the systems when pole shading moves gradually from a panel without SDPO to a panel with SDPO.

To further investigate the performance benefits or losses of the systems, the shading was moved to the un-optimized panels of the SDPO system. In Figure 8, the reference system is gaining around 9% more energy than the SDPO system. While this is counterintuitive, it can be concluded that when un-optimized panels suffer from partial shading, the effect is detrimental to the total system output.

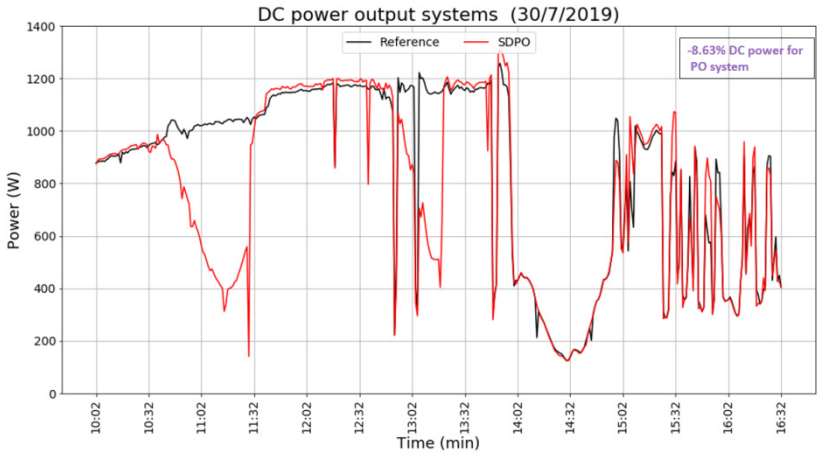

Figure 8. Power comparison of SDPO and reference system when the SDPO system is partially shaded on the un-optimized panels.

3.2. Efficiency Analysis of SDPO

The efficiency of the operating SDPOs was measured directly in the input and output, thus providing accurate data without cable and connection losses (see Figure 9). The European η_{EU} and Californian η_{CEC} efficiency were calculated based on the empirical weight factors [16].

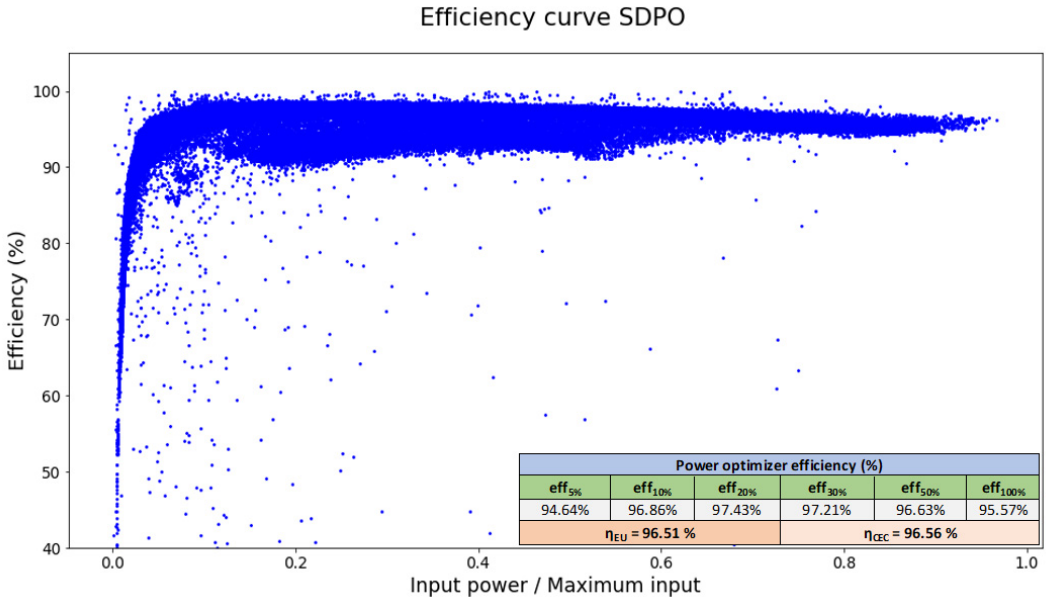

Figure 9. Efficiency curve and calculated η_{EU} and η_{CEC} for the SDPO under test.

The SDPOs under test were rated at 300 W, but the panels that they were connected at were 265 W at STC. Therefore, some data are not available for 100% nominal output efficiency and have been calculated with the maximum values that were measured during the outdoor test. The η_{EU} and η_{CEC} are around 96.5%, but there is a large variation for the low and middle range of the power output. The reason for this efficiency variation can be seen in Figure 10, where the efficiency curve of Figure 9 has been subdivided using color coding according to the normalized input current of the SDPO.

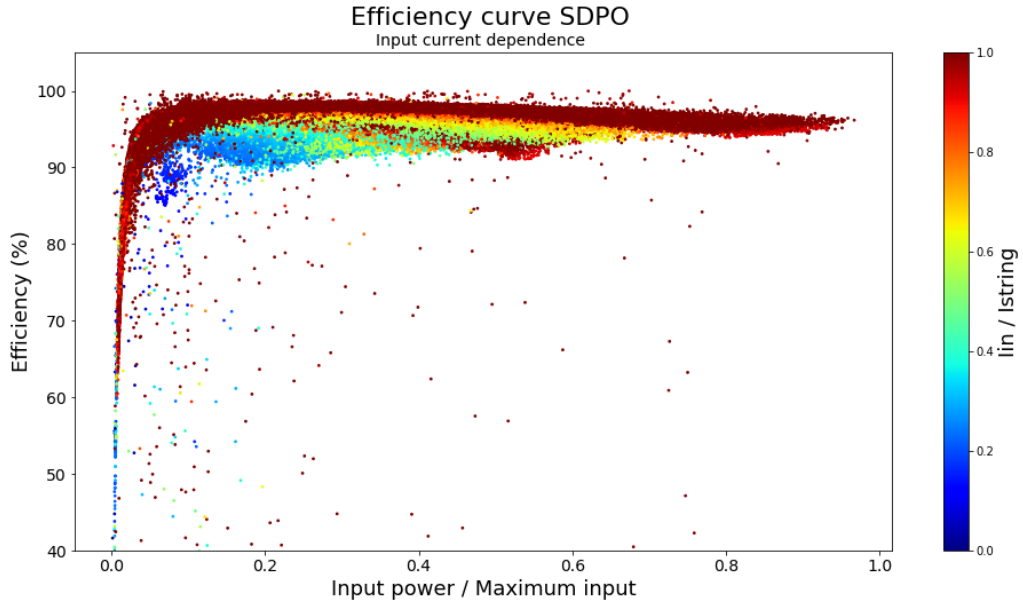

Figure 10. Efficiency dependence of SDPO on input current.

Three groups of current variation have been investigated in Table 1. When the current of the optimized panel matches the string current, the efficiency is relatively high, peaking at 98% and the η_{EU} is 97%. When the panel is lightly shaded and the input current is 90% below the string current, the optimizer starts to adjust it, which leads to η_{EU} being lower, around 95%. Further reducing the input current below 50% of the string current leads to a

further drop of η_{EU} down to 93%. These data were further analyzed and fitted to quadratic curves to acquire mathematical expressions that can be used in the simulation model.

Table 1. SDPO efficiency calculations for different Iin/Istring.

Data	$\mathbf{eff_{5\%}}$	$\mathbf{eff_{10\%}}$	$\mathbf{eff_{20\%}}$	$\mathbf{eff_{30\%}}$	$\mathbf{eff_{50\%}}$	$\mathbf{eff_{100\%}}$	$\boldsymbol{\eta_{EU}}$	$\boldsymbol{\eta_{CEC}}$
All data	94.64%	96.86%	97.43%	97.21%	96.63%	95.57%	96.51%	96.56%
$\mathbf{I_{in} \geq I_{string}}$	94.62%	96.88%	97.69%	97.74%	97.31%	95.71%	96.98%	97.24%
$\mathbf{I_{in} < 0.9 \cdot I_{string}}$	93.54%	95.25%	94.67%	95.28%	95.39%	95.88%	95.32%	95.22%
$\mathbf{I_{in} < 0.5 \cdot I_{string}}$	92.14%	92.54%	93.30%	93.45%	93.27%	93.27%	93.21%	93.23%

3.3. System Performance

The overall performances of the systems were examined for a period of 5 months and were divided into shaded (pole shading) and unshaded periods. For the performance evaluation, the performance ratio [17] was calculated daily for the two systems, taking into account parts of the day that external shading was unevenly affecting the systems.

In the selected period, the PO system outperformed the reference system by 1%, i.e., the average PR of the 5-month period was 1.5% larger for the PO system (see Table 2). When only the shaded period is considered, the SDPO system outperforms the reference system by around 2.5%. However, the reference system still outperforms the SDPO system when no shading is present. In Figure 11, the daily PR can be seen for all periods, while in Table 2, the PR and energy yield can be seen for the DC and AC sides.

Table 2. PR and AC yield for shade, unshaded and mixed period.

		DC Power			AC Power		
		Reference	**SDPO**	**PO Effect**	**Reference**	**SDPO**	**PO Effect**
All data	PR (%) Yield (kWh)	89.21 587.28	90.54 596.06	1.50%	84.55 556.57	85.69 564.11	1.36%
With shade	PR (%) Yield (kWh)	86.42 398.96	88.61 409.06	2.53%	81.85 377.88	83.84 387.04	2.42%
No shade	PR (%) Yield (kWh)	95.76 188.32	95.09 187.00	−0.70%	90.86 178.68	90.05 177.08	−0.90%

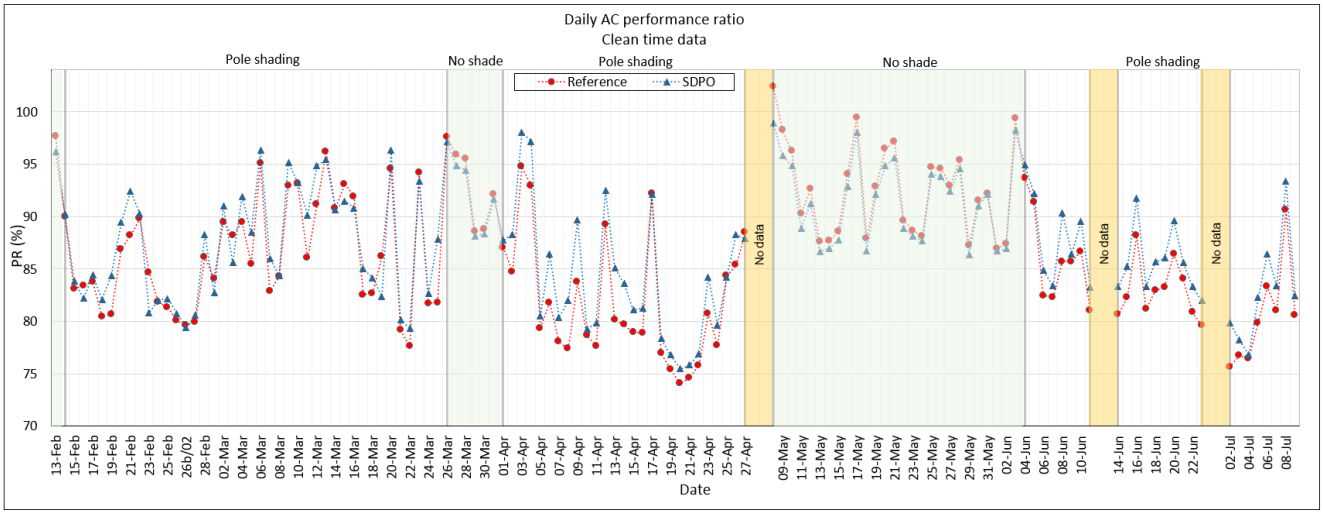

Figure 11. Daily PR of the systems for 6 months.

3.4. Model Validation with Field Test Results

The simulation model, which is explained in detail in previous work [14], was tuned with field test specific power electronic specifications and efficiencies. Moreover, some data was excluded due to uncontrolled shade casting unevenly on the systems (mainly during morning and evening hours). In Figure 12, the measured and simulated power can be seen for a sunny day. Note that the "clean time" taken into account is between 9:42 and 17:40. The deviation between simulated and measured energy throughout the day is 3%.

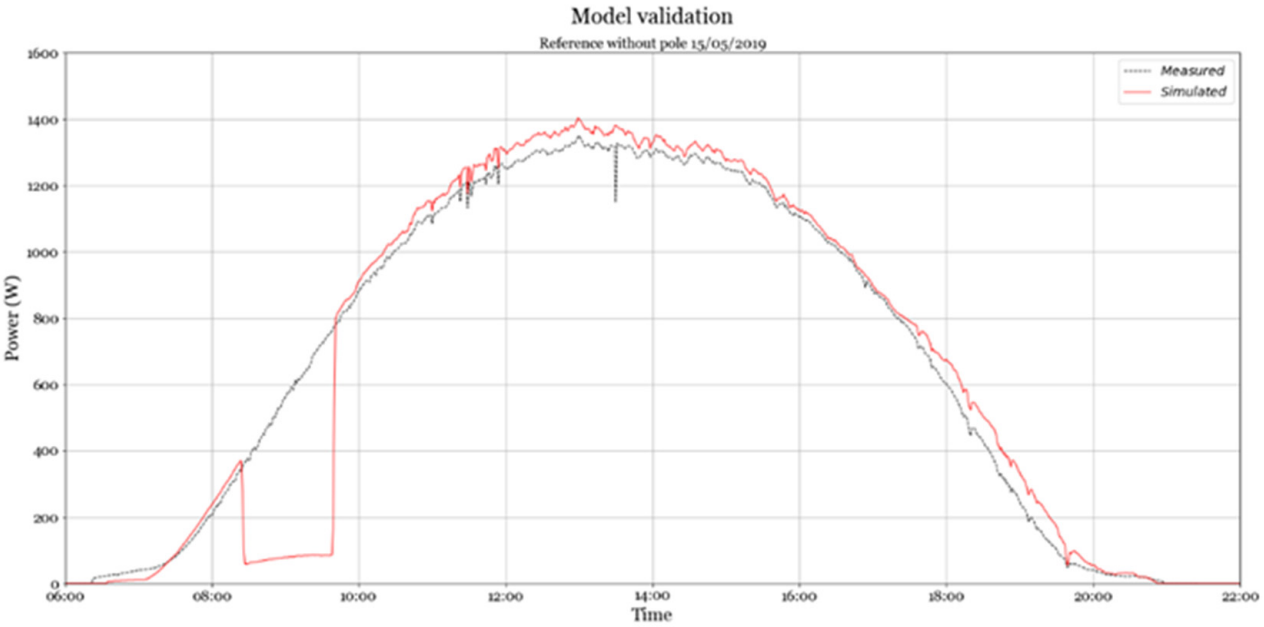

Figure 12. Simulated and measured power output for a sunny day.

In Figure 13, the measured and simulated power can be seen for a mixed day of clouds and sun. The deviation in this case is very small, at around 0.2%.

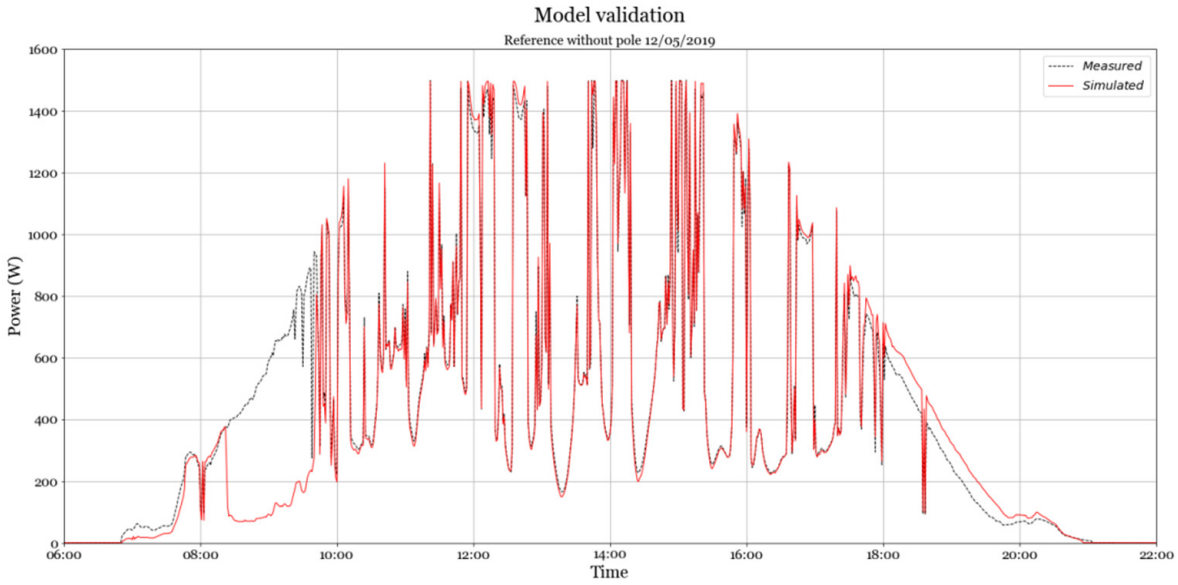

Figure 13. Simulated and measured power output for a mixed day of clouds and sun.

In Figure 14, a set of days is investigated based on the clearness index [18]. The clearness index (Kt) is defined as the ratio of the measured global horizontal irradiance at the test site and the extra-terrestrial irradiance just outside the earth's atmosphere (defined as the solar constant 1367 W/m^2). Days with a clearness index below 0.3 are considered overcast weather days, while days with a clearness index between 0.3 and 0.6 are considered mixed weather days of cloud coverage and sun. For days with a clearness index above 0.6, the weather is classified as sunny.

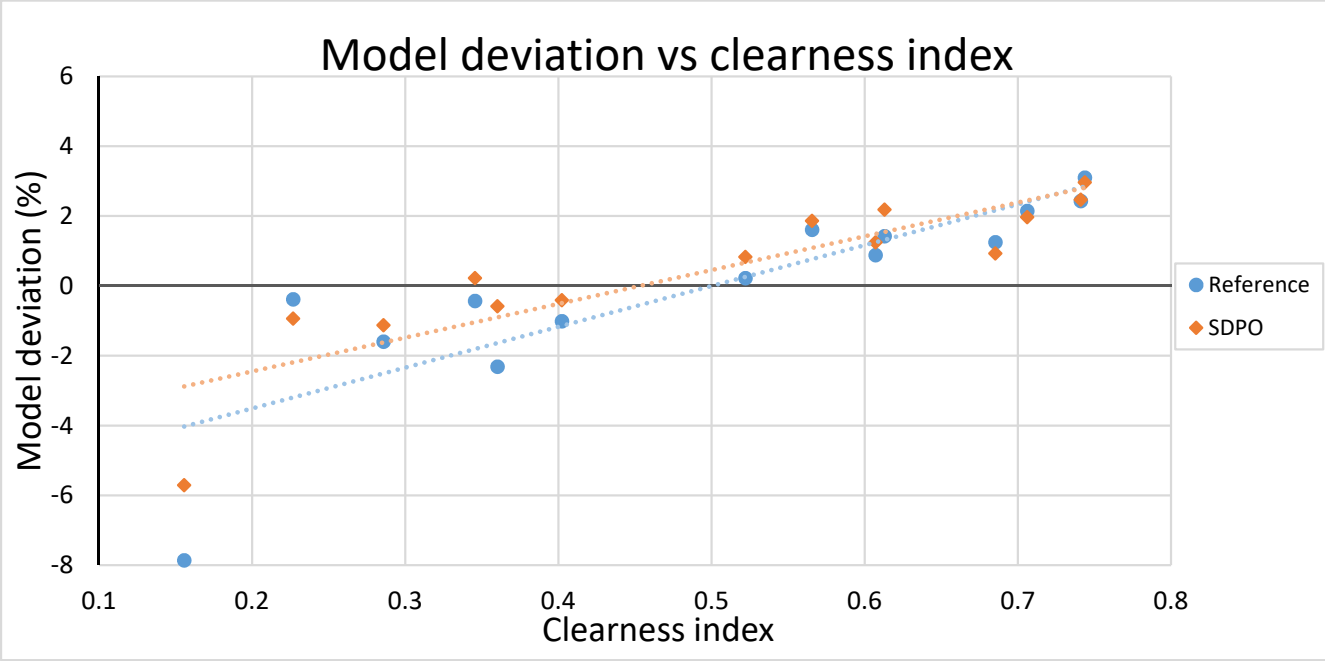

Figure 14. Deviation of simulated and measured energy yield with the clearness index.

A clear correlation between the weather conditions and the model deviation can be deduced from Figure 14. The yield model systematically underestimates the power output on cloudy days (low clearness index) and higher yields for sunny days (clearness index >0.6) are predicted well, while yield values very close to the measured ones can be seen for partly cloudy days. This is probably caused by the irradiance separation model (Reindl2) [19], which calculates the diffuse and direct parts of the irradiance. These irradiance separation models are derived through empirical correlations and are partially valid for certain atmospheric conditions [20]. The higher yields on sunny days could indicate degradation of the solar modules. The panels are from 2013, having operated for 6 or more years outdoors, and should be expected to have suffered a degradation of around 2–4% from their initial power [21]. During partly sunny days, the model behavior counterbalances the effect, leading to a very good approximation of the daily energy yield. Overall, previous research on comparing various yield models has shown acceptable errors and fairly accurate results [22] from predictive yield assessment.

4. Simulation Results for Shading Scenarios

The main focus of this part of the study is to assess the benefits and drawbacks of SDPO in the Dutch-built environment. The typical meteorological year (TMY) irradiation is taken from Meteonorm [23] for Eindhoven. An optimized and non-optimized system of the same size is utilized for detached and row house scenarios.

In Figure 15, the AC-specific yield of the systems is presented in unshaded and shaded scenarios. A variety of obstruction elements present in the built environment are shown together, with variations for different system orientations. Dormers and neighboring buildings seem to create by far the most influential shadow patterns, causing the highest

annual losses of 4–6% and 3–7%, respectively. When evaluating the medium and heavy shading scenario, the losses increase further, up to 7–15% depending on the orientation and building type.

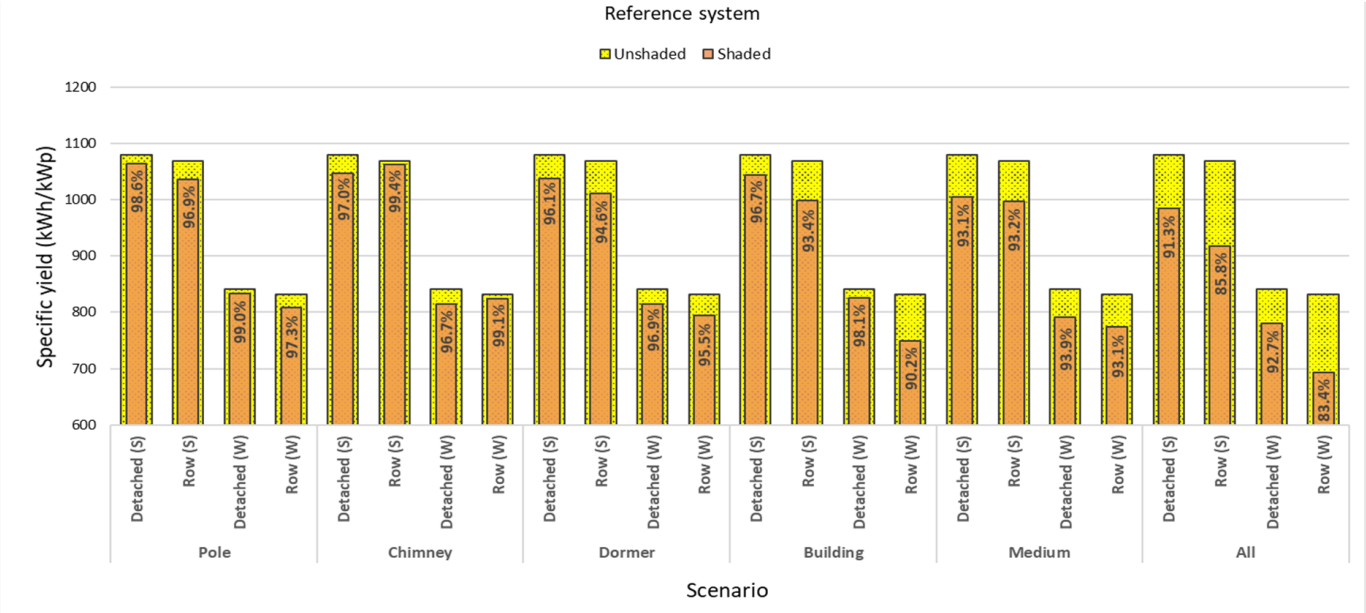

Figure 15. Specific yield and losses compared to unshaded scenarios for the reference system, for two azimuth directions (South, West).

In Figure 16, the losses per system and building type can be seen for a South orientation. The SDPO system seems to operate with lower losses in most scenarios; however, in some scenarios the SDPO system operates with higher losses than the reference system. This occurs due to the fact that the efficiency losses of the SDPOs are dominant during homogeneous shading of the whole system. The variation of optimized panels is different per shade type, starting from two to eight panels. The irradiance losses on the system surface reveal the disproportional losses that occur. For example, an exhaust pipe causes around 0.1% in irradiance losses on the PV system surface on an annual level, but it causes at least 10–12 times more energy loss and is considered the most detrimental shade pattern in these terms. The row house scenario experienced higher losses due to the geometry of the house and the fact that, in row houses, not only is the dormer around the owners system affected, but the neighboring dormers and obstructions also affect system performance. The irradiance losses are even higher in the row house scenario, and mitigation of the SDPOs mostly affects heavy shading scenarios and dormers.

The effects in terms of annual yield losses of SDPO on a system without any shading occurring are presented in Figure 17. A linear dependence of the annual yield losses and the number of SDPOs deployed can be concluded. Moreover, the losses are higher for the row house due to the fact that the PV system rated capacity is smaller than that of the detached house. The losses are associated with the operating efficiency of the SDPOs. It is important to deploy SDPOs only for panels that are affected by shade.

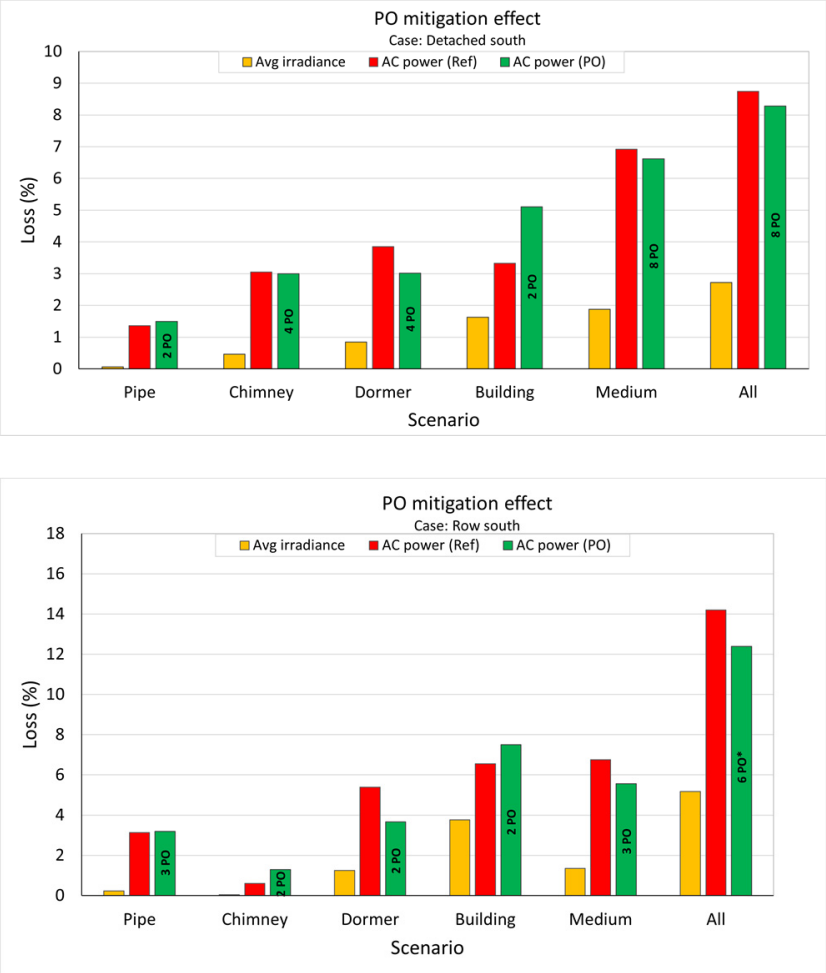

Figure 16. Annual irradiance and AC energy losses per building and system type, for a South orientation. The top displays a detached house and the bottom a row house as defined in the shading scenario Section 2.3.

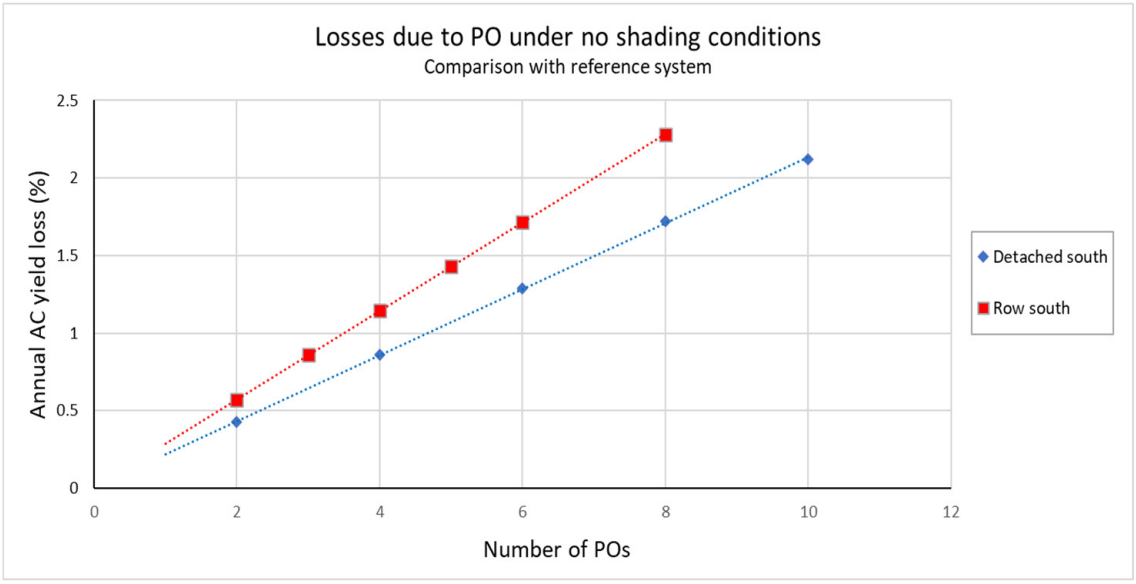

Figure 17. AC yield losses related to SDPO conversion losses in shade-free operation.

5. Discussion

The potential for SDPOs to make up for the yield losses caused by partial shading was investigated in this research. The results obtained from the outdoor field test and the TMY simulations showed limited yield gains in comparison to typical string inverter architecture, and even demonstrated negative gains in some scenarios.

The shading pattern created on the PV system is the most crucial factor regarding its potential for selective deployment. It is determined from the specific nature (dimensions) of the shading objects, their position in respect to the PV system and the incident solar angle, which is relative to the orientation and the location of the PV system. In the case of homogeneous shading on high number of panels of a PV system, like in the case of the "building" scenario, induced losses cannot be mitigated by the use of POs on selected panels, regardless of the position of the shading object, the geographical location, or the system's orientation. Similarly, when yield losses due to shading caused on a PV system are relatively low (a "pole" scenario for the detached house case and a "chimney" scenario for the row house case), selective deployment can lead to lower yields along a TMY than for a single string inverter system. On the other hand, when specific panels are highly affected by shading, as in the case of the "dormer" scenario, the use of power optimizers can be an attractive solution.

One of the key disadvantages of selective deployment of SDPOs is that since the global MPP tracking function of the string inverter is disabled, the reference system performs better when shade affects panels without SDPOs installed. Although the former was verified by the TMY simulations, the results from several different cases examined show that higher yield gains are possible on a PV system by installing POs in fewer panels. There is a trade-off between losses due to local MPP tracking and the gains achieved by avoiding the efficiency losses that can be caused by installing more power optimizers on the system.

6. Conclusions

A model developed for partial shading response of c-Si modules and systems was adapted to accommodate SDPOs. The model was verified with 6 months of real field test data of a reference (non–optimized) system versus that of another system, which included two SDPOs on the partially shade-affected modules. Identical shading patterns were applied on the two systems, resulting in a slight yield benefit from the optimized system.

During operation, SDPOs adjust the module current output to match the string current of the modules. As a result, the module's voltage is reduced. The operating efficiency of the optimizers is relatively high, but it depends on the current output of the module and, thus, the adjustment that the optimizer has to perform. In the conduction state, the optimizer operates at peak efficiency (around 98%), while, when current adjustment is needed, the efficiency drops to 93–95%, depending on the current output of the module. Simulations show that there is a limited energy yield gain on certain shading scenarios, which depend on the shade pattern. A dormer inflicts the highest losses on the system level as a separate shading pattern and is more influential in the row house scenario. Combinations of the shading patterns for the medium and high shading scenarios show a yield benefit of 1–2% for the detached scenario and the row house scenario, respectively.

Overall, SDPOs could be beneficial but should be examined case by case and system by system. A further financial feasibility study should be performed, comparing the energy gains with the investment required for SDPOs.

Author Contributions: K.S. conceived and designed the model, analyzed the data and designed the outdoor field test, K.T. assisted in the model design and adaptation and analyzed data. M.D. assisted in the set-up of the outdoor field test and assisted in data analysis. W.G.J.H.M.v.S. has reviewed the manuscript and data analysis. All authors have read and agreed to the published version of the manuscript.

Funding: This work is partly financed through the Optishade project, with financing from the Topsector Energy subsidies from the Dutch Ministry of Economic Affairs (file nr. TEUE116154).

Institutional Review Board Statement: Not applicable.

Informed Consent Statement: Not applicable.

Data Availability Statement: Not applicable.

Acknowledgments: The authors would like to thank Wiep Folkerts for fruitful discussions.

Conflicts of Interest: The authors declare no conflict of interest.

References

1. European Photovoltaic Industry Association. *Global Market Oulook for Phototovoltaics 2018–2022*; European Photovoltaic Industry Association: Brussels, Belgium, 2018.
2. Psomopoulos, C.S.; Ioannidis, G.C.; Kaminaris, S.D. Chapter 6: Electricity Production from Small-Scale Photovoltaics in Urban Areas. In *Promoting Sustainable Practices through Energy Engineering and Asset Management*; Engineering Science Reference (IGI Global): Hershey PA, USA, 2015; ISBN 978-1-4666-8222-1.
3. Gagnon, P.; Margolis, M.; Melius, J.; Phillips, C.; Elmore, R. *Rooftop Solar Photovoltaic Technical Potential in the United States: A Detailed Assessment*; National Renewable Energy Laboratory: Golden, CO, USA, 2016. Available online: https://www.nrel.gov/docs/fy16osti/65298.pdf (accessed on 15 January 2021).
4. State of the State Report. Solar Panels Could Provide Half of the Dutch Electricity Demand. Deloitte March. 2018. Available online: https://www2.deloitte.com/nl/nl/pages/data-analytics/articles/solar-panels.html (accessed on 15 January 2021).
5. Tang, S.; Xing, Y.; Chen, L.; Song, X.; Yao, F. Review and a novel strategy for mitigating hot spot of PV panels. *Sol. Energy* **2021**, *214*, 51–61. [CrossRef]
6. Pannebakker, B.B.; de Waal, A.C.; van Sark, W.G.J.H.M. Photovoltaics in the shade: One bypass diode per solar cell revisited. *Prog. Photovolt. Res. Appl.* **2017**, *25*, 836–849. [CrossRef]
7. UBIK Solutions. S350 OPTIVERTER. 2019. Available online: https://www.ubiksolutions.eu/s350 (accessed on 10 August 2019).
8. Sinapis, K.; Litjens, G.; van den Donker, M.; Foklerts, W.; van Sark, W.G.J.H.M. Outdoor characterization and comparison of string and module level power electronics under clear and partially shaded conditions. *Energy Sci. Eng.* **2015**, *3*, 510–519. [CrossRef]
9. Soubhagya, K.D.; Deepak, V.; Savita, N.; Nema, R.K. Shading mitigation techniques: State-of-the-art in photovoltaic applications. *Renew. Sustain. Energy Rev.* **2017**, *78*, 369–390. [CrossRef]
10. Suneel, R.P.; Suresh, M. Modelling and performance assessment of PV array topologies under partial shading conditions to mitigate the mismatching power losses. *Sol. Energy* **2018**, *160*, 303–321. [CrossRef]
11. Yingli Solar Panda Series. Available online: https://usa.krannichsolar.com/fileadmin/content/data_sheets/solar_modules/usa/US-YGE-Panda_265_Series.pdf (accessed on 15 January 2021).
12. SMA Solar 1.5 KW Sunny Boy. Available online: https://files.sma.de/downloads/SBxx-1VL-40-DS-nl-40.pdf (accessed on 15 January 2021).
13. High Performance Power Analyzer WT1800. Available online: https://www.yokogawa.com/pdf/provide/E/GW/Bulletin/0000024844/0/BUWT1800-00EN.pdf (accessed on 15 January 2021).
14. Sinapis, K.; Tzikas, C.; Litjens, G.; van den Donker, M.; Folkerts, W.; van Sark, W.G.J.H.M.; Smets, A. A comprehensive study on partial shading response of c-Si modules and yield modeling of string inverter and module level power electronics. *Sol. Energy* **2016**, *135*, 731–741. [CrossRef]
15. CBS. Vier op de Tien Huishoudens Wonen in Een Rijtjeshuis. 2016. Available online: https://www.cbs.nl/nl-nl/nieuws/2016/14/vier-op-de-tien-huishoudens-wonen-in-een-rijtjeshuis (accessed on 14 November 2018).
16. European or CEC Efficiency. Available online: https://www.pvsyst.com/help/inverter_euroeff.htm (accessed on 15 January 2021).
17. Nils, H.R.; Björn, M.; Alfons, A.; van Sark, W.G.J.H.M.; Klaus, K.; Christian, R. Performance ratio revisited: Is PR > 90% realistic? *Prog. Photovolt. Res. Appl.* **2012**, *20*, 717–726. [CrossRef]
18. Lai, C.S.; Li, X.; Lai, L.L.; McCulloch, M. Daily clearness index profiles and weather conditions studies for photovoltaic systems. *Energy Procedia* **2017**, *142*, 77–82. [CrossRef]
19. Reindl, D.T.; Beckman, W.A.; Duffie, J.A. Diffuse fraction correlations. *Sol. Energy* **1990**, *45*, 1–7. [CrossRef]
20. Sun, X.; Bright, J.M.; Gueymard, C.A.; Bai, X.; Acord, B.; Wang, P. Worldwide performance assessment of 95 direct and diffuce clear sky irradiance models using principal component analysis. *Renew. Sustain. Energy Rev.* **2021**, *135*, 110087. [CrossRef]
21. Ababacar, N.; Abdérafi, C.; Abdessamad, K.; Cheikh, M.F.; Kébé, P.A.; Ndiaye, V.S. Degradations of silicon photovoltaic modules: A literature review. *Sol. Energy* **2013**, *96*, 140–151.
22. Psomopoulos, C.S.; Ioannidis, G.C.; Kaminaris, S.D.; Mardikis, K.D.; Katsikas, N.G. A Comparative Evaluation of Photovoltaic Electricity Production Assessment Software (PVGIS, PVWatts and RETScreen). *Environ. Process.* **2015**, *2* (Suppl. 1), 175–189. [CrossRef]
23. *Meteonorm*; Irradiation data; Meteotest AG: Bern, Switzerland, 2015; Retrieved 14 February 2019.